Design, construction, and performance of VIRUS-P: the prototype of a highly replicated integral-field spectrograph for HET [*]

Gary. J. Hill[a†], Phillip J. MacQueen[a], Michael P. Smith[a], Joseph R. Tufts[b], Martin M. Roth [c], Andreas Kelz [c], Joshua J. Adams[a], Niv Drory [d], Frank Grupp[d], Stuart I. Barnes[a], Guillermo A. Blanc[a], Jeremy D. Murphy[a], Werner Altmann [e], Gordon L. Wesley[a], Pedro R. Segura[a], John M. Good[a], John A. Booth[a], Svend-Marian Bauer [c], Emil Popow [c], John A. Goertz[a], Robert D. Edmonston[a], Christopher P. Wilkinson[a]

[a] McDonald Observatory and Department of Astronomy, The University of Texas at Austin, 1 University Station C1402, Austin, TX 78712-0259, USA

[b] Las Cumbres Observatory, 6740 Cortona Dr., Ste. 102, Goleta, CA 93117 USA

[c] Astrophysikalisches Institut Potsdam, An der Sternwarte 16, 14482 Potsdam, Germany

[d] Max-Planck-Institut für Extraterrestriche-Physik, Giessenbachstrasse, D-85748 Garching b. München, Germany

[e] Konstructionsburo Werner Altmann, Sonnenstr. 41, Haselbach, 94113 Tiefenbach, Germany

ABSTRACT

We describe the design, construction, and performance of VIRUS-P (Visible Integral-field Replicable Unit Spectrograph – Prototype), the prototype for 150+ identical fiber-fed integral field spectrographs for the Hobby-Eberly Telescope Dark Energy Experiment (HETDEX[‡]). VIRUS-P was commissioned in 2007, is in regular service on the McDonald Observatory 2.7 m Smith telescope, and offers the largest field of any integral field spectrograph. The 246-fiber IFU uses a densepak-type fiber bundle with a 1/3 fill factor. It is fed at f/3.65 through a telecentric, two-group dioptric focal reducer. The spectrograph's double-Schmidt optical design uses a volume phase holographic grating at the pupil between the articulating f/3.32 folded collimator and the f/1.33 cryogenic prime focus camera. High on-sky throughput is achieved with this catadioptric system by the use of high reflectivity dielectric coatings, which set the 340-670 nm bandwidth. VIRUS-P is gimbal-mounted on the telescope to allow short fibers for high UV throughput, while maintaining high mechanical stability. The instrument software and the 18 square arcmin field, fixed-offset guider provide rapid acquisition, guiding, and precision dithering to fill in the IFU field. Custom software yields Poisson noise limited, sky subtracted spectra. The design characteristics are described that achieved uniformly high image quality with low scattered light and fiber-to-fiber cross talk. System throughput exceeds requirements and peaks at 40%. The observing procedures are described, and example observations are given.

Keywords: Telescopes: Hobby-Eberly Telescope, Astronomical instrumentation: Spectrographs: VIRUS, Dark Energy

1. INTRODUCTION

Large targeted surveys of continuum-selected objects are now becoming the norm, and have greatly increased our understanding in many areas of astronomy. Surveys of the emission-line universe, however, are limited currently to wide field imaging with narrow band filters or to narrower fields with Fabry-Perot etalons. Integral field (IF)

[*] The Hobby – Eberly Telescope is operated by McDonald Observatory on behalf of the University of Texas at Austin, the Pennsylvania State University, Stanford University, Ludwig-Maximillians-Universität München, and Georg-August-Universität, Göttingen

[†] G.J.H.: E-mail: hill@astro.as.utexas.edu

[‡] http://hetdex.org/

spectrographs offer a huge gain over these techniques, providing much greater sensitivity, or much greater wavelength coverage, respectively. The current generation of IF spectrographs are well-adapted to arcminute-scale fields of view, with several thousand spatial elements, and adequate spectral coverage for targeted observations of individual extended objects. They have the grasp to detect simultaneously of order 0.5 million (spectral x spatial) resolution elements.

In order to undertake large-scale surveys for emission-line objects, much greater field coverage is needed. Narrow band imaging can now cover large area, but require spectroscopic follow up, and still do not probe sufficient volume to detect rare objects or to be cosmic variance limited. Wide-field IF spectroscopy is hard to achieve without a large multiplexing factor, so we have embarked on a program to produce an instrument that uses large-scale replication to create a unique astronomical facility capable of spectroscopic surveys of hundreds of square degrees of sky. The instrument is the Visible Integral-field Replicable Unit Spectrograph (VIRUS)[1,2,3], a simple, modular integral field spectrograph that is to be replicated 150-fold, to provide an order of magnitude increase in grasp over any existing spectrograph, when mounted on the upgraded Hobby-Eberly Telescope (HET)[4].

The traditional astronomical instrument has a monolithic design and is a one-off prototype, where a large fraction of the cost is expended on engineering effort. When compared to monolithic instruments, there are cost savings from creating several copies of a spectrograph to gain multiplex advantage, because the components are less expensive and the engineering is simplified. Several current instruments use small-scale replication to achieve multiplex advantage. These include the DEIMOS[5] and VIMOS[6] imaging spectrographs with two and four copies of each, respectively, within single structures. The MUSE[7] instrument for ESO VLT will field-slice a 1 arcmin. square field into 24 duplicated spectrographs. VIRUS makes the next step, and exploits industrial-scale replication, which we (arbitrarily) define to be in excess of 100 units. We build upon the concepts laid out in Refs. 1,2,3, & 8, where we concluded that industrial replication offers significant cost-advantages when compared to a traditional monolithic spectrograph, particularly in the cost of the optics and engineering effort. This concept breaks new ground in optical instruments, and appears to be a cost-effective approach to outfitting the coming generation of ELTs, for certain instrument types.

The motivation for VIRUS is the Hobby-Eberly Telescope Dark Energy Experiment (HETDEX[9]), which will map the spatial distribution of about 0.8 million Lyα emitting galaxies (LAEs) with redshifts $1.9 < z < 3.5$ over 420 sq. deg. area (9 Gpc^3). This dataset will constrain the expansion history of the Universe to 1% and provide significant constraints on the evolution of dark energy. The advantage of an IF spectrograph for this project is that the tracer galaxies are identified and have their redshifts determined in one observation.

Development of VIRUS is following a standard production model. A prototype of the unit spectrograph (VIRUS-P) has been constructed and is the subject of this paper. It is being followed by a pre-production prototype, where value engineering is being used to reduce costs before entering production. The motivation for building VIRUS-P is to provide an end-to-end test of the concepts behind HETDEX, both instrumental and scientific. Here we describe the design, construction and performance of VIRUS-P. Construction and testing of the prototype has verified the opto-mechanical design, the throughput, the sensitivity, and demonstrated the utility of such an instrument for surveys of emission-line objects. It has also served as a test-bed for the software development needed for analyzing the data from the full VIRUS array. The parallel nature of VIRUS means that the prototype can be used to develop the final software pipeline. VIRUS-P has already been used to conduct a pilot survey of Ly-α emitting galaxies in support of the HETDEX project, and for several other projects. VIRUS-P is also designed to be a facility instrument on the McDonald 2.7 m Smith Reflector, and it dominates the dark-time usage on that telescope.

2. DESIGN REQUIREMENTS

The design of VIRUS flows strongly from the requirements for HETDEX, to maximize the number of LAEs detected in a set observing time, and to span sufficient redshift range to survey the required volume. These science requirements flow down to the following technical requirements for VIRUS-P:

- Coverage of $\Delta z \sim 2$ and coverage into the ultraviolet to detect LAEs at the lowest possible redshift. VIRUS-P is designed for $340 < \lambda < 570$ nm or $1.8 < z < 3.7$
- Resolution matching the linewidth of LAEs (R~800) to maximize detectability.
- Minimum throughput on sky (including atmosphere) ranging between 5% at 350 nm and 15% at 450 nm to reach sensitivity of 3-4e-17 erg/cm^2/s in 20 minutes on HET.

- Low read noise detector (~3 electrons) to achieve sky-background dominated observations in 300 seconds
- High stability to ambient temperature variations, though not to gravity variations since the VIRUS modules will be fixed on HET.
- Simple, inexpensive design.

These principles guided the development of VIRUS-P, and we will discuss the performance of the instrument in light of these requirements in section 4.

3. DESIGN DEVELOPMENT

The VIRUS unit consists of a fiber-coupled IFU feeding a single, simple spectrograph. The basic parameters of VIRUS-P are given in Table 1 and the layout is shown in Figure 1. It mounts at the f/9 bent cassegrain focus, of the McDonald 2.7 m, fed by a f/3.65 focal reducer. It is supported within a gimbal in order to mimic the mounting on the HET, where the instrument will be fixed with respect to gravity but will see the full range of operating temperatures. The design is optimized for stability against temperature changes. The instrument consists of three basic sub-units: the fiber IFU, the collimator/grating assembly, and the camera assembly. In VIRUS-P, the collimator and grating pivot about a horizontal axis passing through the plane of the grating, to allow reconfiguration of the instrument for different wavelength ranges and resolving powers and to shift the blaze of the volume phase holographic grating. Gratings are interchangeable to provide flexibility for different scientific applications. The final VIRUS units will have fixed formats, but will have the capability to swap dispersers. The instrument mounts within a light-tight box that incorporates a lead-screw and clamps to adjust the tilt of the collimator with respect to the camera. The camera is an f/1.35 vacuum Schmidt design with a 2k x 2k @ 15 μm pixel CCD at its internal focus. VIRUS-P was delivered in October 2006 and has been in use on the 2.7 m since then. In September 2007 the upgrade of the detector to a modern Fairchild 3042 device and the deployment of an improved grating resulted in a significant improvement in blue throughput and much lower read noise, aiding sensitivity.

Table 1: basic properties of VIRUS-P

IFU	246 fibers, each 200 μm diameter or 4.16 arcsec. diameter on the McDonald 2.7 m. Square format 1.7x1.7 sq. arcmin. area, 1/3 fill-factor, hexagonal pack fed at f/3.65 with a focal reducer. Fiber diameter is 1.23 arcsec. on the current HET, fed at f/3.65
Collimator	accepts f/3.32, folded reverse-Schmidt reflective design, without corrector
Camera	f/1.33 Schmidt with 2k x 2k 15 μm pxl CCD at internal focus. Aspheric corrector plate and field flattener. Fiber reimaged to approximately 4.9 pixels
Disperser	831 l/mm VPH grating gives 340-570 nm simultaneous coverage at R~850; dispersion 0.11 nm/pixel 0.56 nm per resolution element

3.1 Optical Design and Fabrication

In the course of developing the prototype of the VIRUS module, we first investigated refractive optical designs with beam sizes between 75 and 100 mm (Ref. 3). The field angles required to accept the number of fibers, coupled with the desire for coverage into the ultraviolet, proved difficult for designs without large numbers of elements and use of calcium fluoride. Evaluation of the throughput, the weight, and the cost of these designs led us to investigate catadioptric alternatives, where we knew we could obtain high throughput at relatively low cost. Comparison of real designs showed that when glass absorption and anti-reflection coatings were taken into account, the refractive designs did not have a significant throughput advantage over those with mirrors. This approach was not our first line of investigation mainly because it necessitates a cryogenic camera with the detector at an internal focus, but such designs are pan-chromatic and can be very efficient, as demonstrated by the camera for the HET Low Resolution Spectrograph, for example[10]. This is particularly true of designs with limited bandwidth where very high reflectivity coatings can be applied.

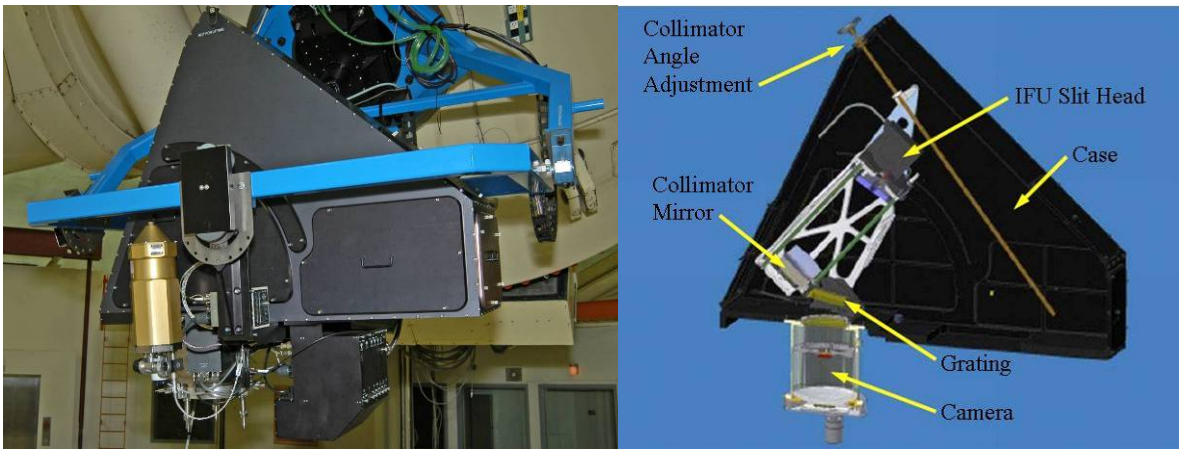

Figure 1. The photograph on the left shows VIRUS-P installed on the Harlan J. Smith telescope. The blue structure is a gimbal to maintain orientation with respect to gravity. The illustration in the middle shows the interior components which are fed by an IFU that contains 246 fibers with 200 μm diameter cores. For reference the size of the camera and collimator modules is about 0.6 m. The black case incorporates an adjuster of the collimator angle for wavelength range adjustment.

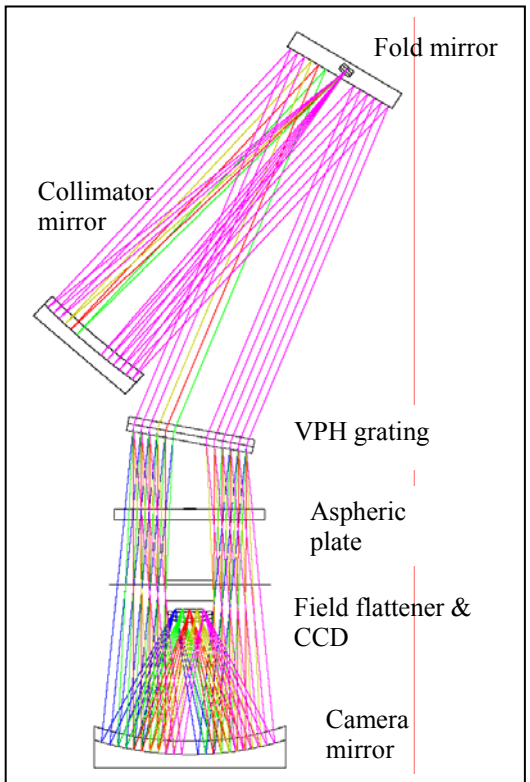

Figure 2: Optical design of the VIRUS-P spectrograph. The standard setup is shown, covering 340 – 570 nm at R=900. The linear fiber input is arrayed out of the page.

The final optical design for VIRUS-P is shown in Figure 2, and the spot diagrams in Figure 3. The input focal ratio is f/3.62 and the camera focal ratio is f/1.33. Details of the prescription will be given elsewhere. The collimator is a reverse-Schmidt, where the input fibers are arrayed pointing perpendicular to the spherical collimator mirror so as to create an axis-less system. A cylindrical lens is coupled to the fibers to provide immersion of the ends with an AR coated exit face for maximum efficiency. A fold mirror is introduced for compactness and to allow flexibility in the design of the integral field unit interface. The disperser is a volume phase holographic grating with 831 fringes/mm sandwiched between fused silica plates. The camera is a Schmidt with aspheric corrector plate and an aspheric surface on the back side of the field flattener lens, both of fused silica. It was found that the correction for both the collimator and camera could be achieved with a single asphere on the camera corrector, which also acts as the window for the vacuum housing of the camera. This design achieves excellent images, far superior to those achieved with the refractive designs we investigated. Modeling of data frames has included the convolved image quality and distortion predicted from the optical design and shows well-separated spectra from the individual fibers, as expected from the excellent image quality shown in Fig. 3. Good separation of spectra is important in reducing cross-talk and enabling straight-forward extraction of the individual spectra.

VIRUS is designed to be fiber fed at f/3.65, and allows for some focal ratio degradation (FRD), as the collimator accepts f/3.32 for which it produces a pupil of 125 mm diameter. The camera is designed to accept this clear aperture. Fiber tests (below) show that more than 95% of the light falls within this pupil and that the radial scrambling (responsible for FRD) is very small at this fast input f-ratio. As a result the central obstruction of the input is largely maintained, reducing the disadvantage of an internal Schmidt camera used with fibers. This excellent FRD performance has also been demonstrated for a fiber length of 15 m (Ref. 11).

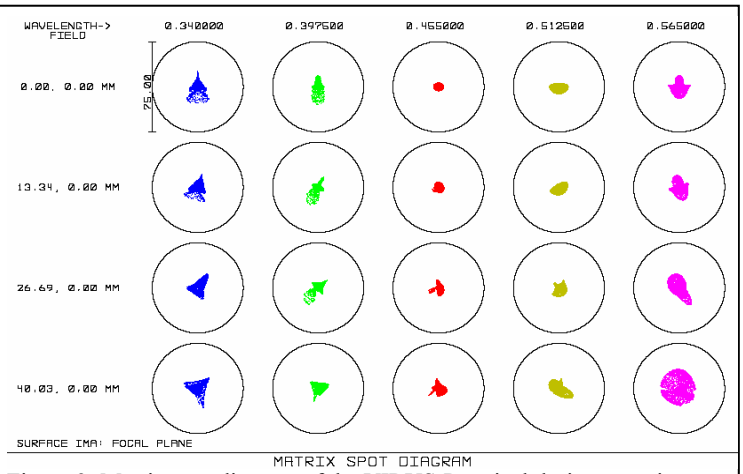

Figure 3: Matrix spot diagram of the VIRUS-P optical design covering the entire focal surface (symmetrical about the top row). The circles are 75 microns diameter, the scale to which a 200 μm fiber core is reimaged. Wavelengths range from 340 to 565 nm in this figure, but image quality is maintained for different wavelength settings over the 340-670 nm bandwidth of the instrument.

The fused silica substrate mirrors were manufactured by Harold Johnson Optical Labs. The spherical mirrors were designed with spherical rear surfaces to minimize weight and allow mounting on invar bosses at the rear of each mirror. This cantilevered design is very simple, and the mirrors are mounted to the aluminum frame with a central shoulder screw and a second to prevent rotation. Figure 4 shows the mirrors prior to coating. They were coated with a high efficiency dielectric mirror coating by ZC&R achieving an average >98.5% reflectivity over 340-670 nm with no dips below 95%. The aspheric elements were manufactured by Asphericon (Jena) using CNC grinding/polishing, which easily met the specifications on figure. The design works far from the diffraction limit, so few-wave errors are acceptable and are now within the capabilities of mass-production for 180 mm diameter.

The catadioptric design of VIRUS allows other modes with higher resolving powers and different wavelength coverage[6]. One of the aims of VIRUS-P is to test such modes, and the instrument can cover wavelengths as red as 670 nm and provide resolving powers as high as R=4000, by substituting the grating for one with higher dispersion and setting the collimator and grating angles appropriately. Angles of incidence as high as 45 degrees onto the grating are allowed by the mechanical design. While these options open up interesting observing projects for VIRUS-P, an evaluation of the science drivers for a fully reconfigurable VIRUS, in light of the technical challenges, has led us to adopt a standard fixed low resolution format for the final VIRUS units rather than incur the complexity, volume, and cost of allowing all units to be reconfigured.

Certain baffles are key to the suppression of scattered light in this design. The most important ones are at the grating, at the entrance to the camera, in the plane of the detector and at the camera mirror.

3.2 Gratings

Volume phase holographic (VPH) gratings offer high efficiency and low cost. The standard setup originally envisioned for HETDEX employs a volume phase holographic (VPH) grating with 831 fringes per mm, and Bragg angle close to 11 degrees. The clear aperture of the grating is 130 mm. We have undertaken tests of small and full size gratings from Wasatch Photonics and Kaiser Optical Systems International (KOSI), using a custom automated test-bench that can fully characterize a grating over a range of input and output angles. This test bench will be used to evaluate the gratings for the full VIRUS array, and is described elsewhere in these proceedings[12]. Performance in the ultraviolet has been enhanced by reducing the angle of incidence to about 9.5 degrees to shift the blaze to the UV. Angle changes of the grating at fixed collimator angle have little effect on the wavelength range, so tilting the grating provides an independent free parameter in tuning the throughput as a function of wavelength. This is equivalent to tilting the fringes in the grating, but allows standard setups and processing for untilted fringes to be employed, reducing cost. The ability to independently tilt the angle of the collimator and grating in VIRUS-P has allowed the instrument to be set up for optimal performance for the grating, as measured in the lab.

3.3 Integral Field Unit

It is essential to couple VIRUS to the HET with fibers due to the weight and space constraints at the prime focus of the telescope. In addition, the variable effects of the changing pupil illumination of HET during a track are mostly removed by azimuthal scrambling along a fiber, producing much greater stability in the data calibration than is possible with an imaging spectrograph. Fiber IFUs can utilize microlens arrays, providing close to 100% fill-factor[13], or be of the simpler "densepak" type[14]. For VIRUS we have elected to use the densepak type of bare fiber bundle to maximize

throughput and minimize cost[15]. The primary advantage of lenslets is in coupling the slower f/ratios of typical foci to the fast ratio required to minimize focal ratio degradation[16], and such IFUs are ideal for retro-fitting existing spectrographs. Lenslets do not provide perfect images, however, so if there is flexibility to choose the input f/ratio to the fibers and if the fill-factor can be tolerated, trading it against total area, the bare bundle provides the best efficiency[2]. We use a fill factor of 1/3, with the fibers in a hexagonal close pack, and dither the IFU arrays through three positions to fill the area. Note that if the f/ratio of the microlens case is the same as the f/ratio from the telescope in the bare-fiber case, and the lenslets subtend the same area on the sky as the bare fibers, then the fill-factor of the densepak type array is exactly offset by the larger area that the bundle covers per exposure. So in the case where maximum areal coverage is required, the bare bundle is the preferred solution[2].

HET has a fast focal ratio in order to couple efficiently to fibers, and VIRUS uses a densepak-type IFU. The HET site has a median seeing of 1.0 arcsec. FWHM, and we initially adopted 1 sq. arcsec. per fiber (200 μm core diameter) on the upgraded HET as an optimal compromise between sensitivity and area coverage. Subsequent analysis of the trade off between areal coverage and sensitivity indicates that larger fibers are preferred for HETDEX to maximize the number of detected LAE galaxies. As a result, 1.5 arcsec. (265 μm) diameter is the requirement for the production VIRUS units. The current HET corrector is f/4.65, but the future wide-field corrector will have f/3.65. The optics of VIRUS can accommodate an f/ratio of f/3.32, allowing a degree of focal ratio degradation. Detailed testing[11] of fibers from Polymicro (FB200220240), CeramOptec (UV200/220P), and FiberTech (AS200220UVPI) shows that this f-ratio accepts over 95% of the light input at f/3.65.

Figure 4: Fiber IFU development. The left panel shows the assembly of the AIP fiber head with a matrix of fused silica capillary tubes clamped in a stainless steel fixture and then filled with fibers. The middle panel shows the same bundle after gluing with Epotek 301-2 low-shrinkage epoxy, cutting and polishing. The head has very small size allowing IFUs to be spaced on the focal surface with a fill-factor as tight as ¼. The right hand panel shows the head of the bundle produced by Fibertech, where the fibers were set into drilled stainless steel plates, bonded and polished.

Table 2: Fiber IFU Development Status

Bundle	Length	N fibers	fiber dia	Status	Manufacturer	Notes
VP1	4.5 m	247 (+ 8 cal)	200 μm	In use on 2.7m telescope since 2006	AIP	Polymicro FBP
VP2	15 m	246	200 μm	Tested on HET and in use on 2.7 m	Frank Optics & AIP	Polymicro, FiberTech, Ceram Optec fibers
VP3	15 m	216	250 μm	In manufacture due July 2008	Ceram Optec	Larger fibers to test HETDEX mode on HET
VPX	4 m	246	200 μm	Requires slit end	FiberTech	Will use for tests

The VIRUS-P IFU uses 200 μm core-diameter Polymicro FBP fiber and has 246 fibers arrayed in a hexagonal pack with a 1/3 fill-factor. Anti-reflection coated cover plates mounted to the fiber ends with index-matched optical couplant ensure maximum throughput. This layout is most optimal for covering area, since a dither-pattern of three exposures exactly fills the field of the IFU, while maximizing the efficiency.

On the 2.7 m at f/3.65, the 200 μm fiber cores subtend 4.1 arcseconds, and the IFU covers 3.5 sq. arcminutes. While the fibers are large, projected on the sky, the IFU covers the largest area of any current IF spectrograph and this results in great sensitivity for wide area surveys and particularly for low surface brightness emission. The prototype incorporates adjustment of the collimator angle and the grating angle, as well as allowing different gratings to be employed. These features will not be incorporated into the final VIRUS modules, which are fixed in order to ensure simplicity and to save space and money. It does however test all the features of the instrument needed for the full VIRUS array.

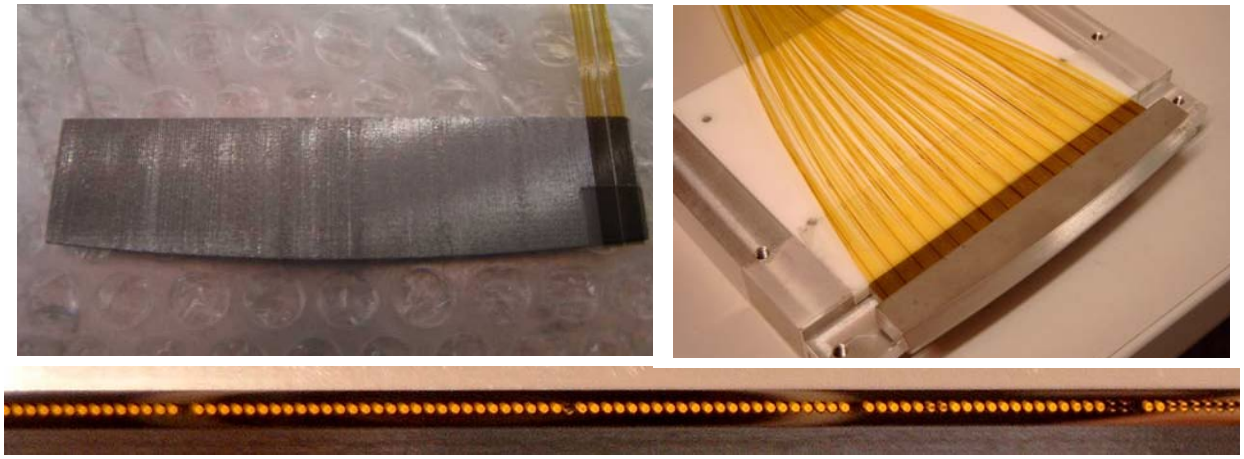

Figure 5: The pseudo-slit output of the IFU bundles. VP1 is shown on the left and VP2 on the right. The fibers are arrayed on a precision grooved plate that sets the spacing and angle between fibers. The fibers are arrayed perpendicular to the back surface of a cylindrical lens bonded to the convex surface of the plate. In VP1 the fibers were pre-polished and then assembled, while in VP2 the slit was polished after assembly to the required cylindrical shape. The pitch of the fibers is 320 μm, resulting in a separation of 7.8 pixels on the CCD.

Development of the prototype IFUs at AIP[15] and UT[11] has explored several ways of setting up the required matrix of fibers at the input end. Setting up a matrix fused silica capillary tubes to set the spacing proved very successful. The fibers are easily threaded into tubes with only 5 μm clearance on the diameter, and these arrays were measured to have final fiber position errors of less than 5 μm rms. This is well within the requirements. One fiber bundle (designated VP1) has been assembled with Polymicro FBP fibers, using this method at AIP. A second bundle of length 15 m has been manufactured by Frank Optic Products in Berlin using the capillary technique and a variety of fiber types. A third long IFU cable is being assembled by Ceram Optec using a micro-drilled ceramic block to locate the fibers at the input. Another fiber bundle has been produced by FiberTech using drilled aperture plates of stainless steel. Table 3 lists the different development bundles and their basic properties. Fig. 4 shows the input ends of the two bundles. Anti-reflection coated fused silica cover plates are bonded to the polished surface of each IFU with index-matching couplant to minimize insertion losses. Measurements of FRD and throughput before and after immersing the ends demonstrate marked improvement for many fibers, and results in very uniform throughput variation[11].

At the output of the bundle, the fibers are arrayed in a line, immersed against the curved back face of a cylindrical lens, and fanned out with their axes pointing perpendicular to the collimator mirror (and to the lens). This layout allows collimation of the beam to be achieved with only one spherical mirror, leading to a very efficient design. The spacing of 320 μm with 0.043 degrees between fibers is achieved by bonding the fibers to a monolithic groove plate of stainless steel. Fig. 5 shows the plate with test fibers bonded in place. Table 2 summarizes the status of the fiber IFU development.

3.4 Collimator and Grating Unit Mechanical Design

The VIRUS prototype is required to operate with high stability under a wide range of temperature from -5 to +25 degrees Celsius. The instrument is specified to not require recalibrating for the positions of the fiber images over the temperature range encountered during a night. This corresponds to shifts smaller than 0.5 pixels (1/10 of a resolution element) at the detector for 5 degrees Celsius temperature change. Stability of image quality throughout the range of angles of the collimator and grating is required, but repeatability of setup is only at the resolution element level. The final design for VIRUS on HET may not require such a constraint if the units are housed in an environmentally controlled housing, but we decided to impose the strictest requirements on the prototype in order to prove engineering concepts that might be required for the final instrument. In addition, we designed the prototype to test all possible modes of the instrument, including a range of resolving powers and wavelengths, even if these will not be options for the majority of VIRUS units, in practice.

The mechanical design is shown in Figure 1 and is discussed in more detail in Ref. 17. The instrument has a collimator and disperser module and a camera with a cryogenic detector head at its internal focus. The majority of the collimator parts are of Aluminum with Invar metering rods maintaining the spacing between the collimator mirror and the IFU output. Three invar rods act as rails to which the optics are mounted, with simple adjustments and clamps. The rods are bolted at one end to the IFU reference plate of Aluminum (to which the IFU slit head mounts), and at the other to disk flexures mounted in an aluminum plate. This setup effectively allows the structure to have the CTE of aluminum in all dimensions except the optical axis where invar is needed to maintain focus. Tests show that the instrument is extremely stable, so this design has proven successful.

Adjusters for the collimator mirror and flat mirror tip-tilt and piston are very simple, consisting of spherical bushings with slots and orthogonal clamps to lock the position. There are three for each mirror. The bushings slide on the invar rods and are adjusted with threaded nuts against springs. The resolution of adjustments is very fine, and the clamps are easy to use in spite of their simplicity and low cost.

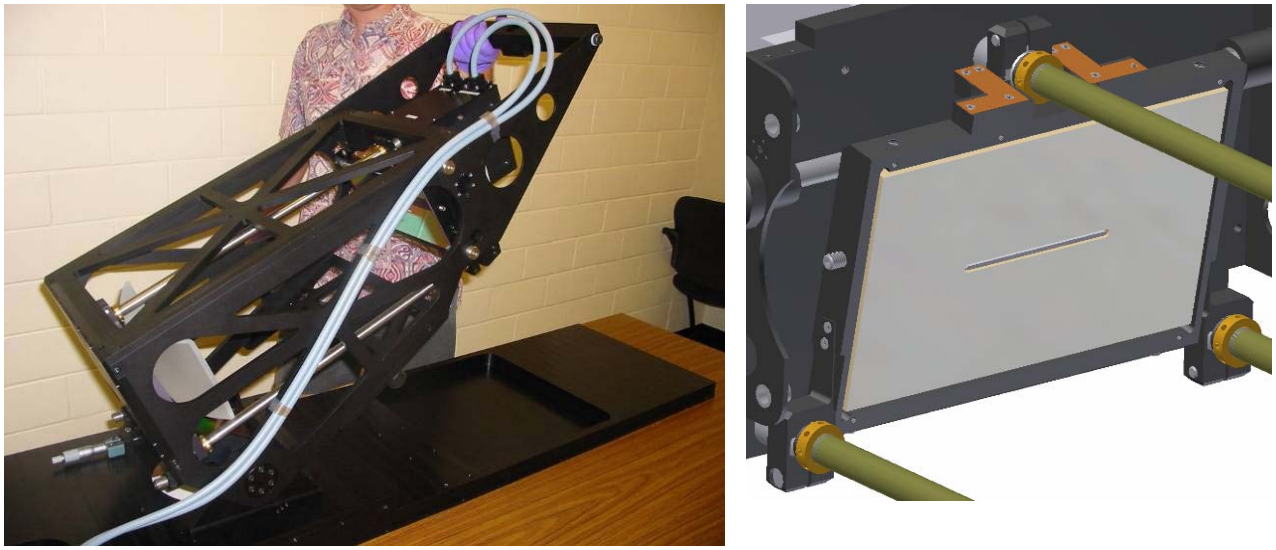

Figure 6: Details of the mechanical design of the collimator/grating assembly of VIRUS-P. The assembly is shown with IFU mounted on the left. On the right, a detail of the mount for the fold flat mirror is shown. Note the slot in the mirror through which the light from the fibers diverges. The cell allows this slot to be aligned with the IFU head, and the three adjusters mount the cell to the invar rods that meter the assembly. Each adjuster has a split spherical bushing sliding on the invar rod, and clamped in position. A flexure at the top mount prevents over-constraint of the system.

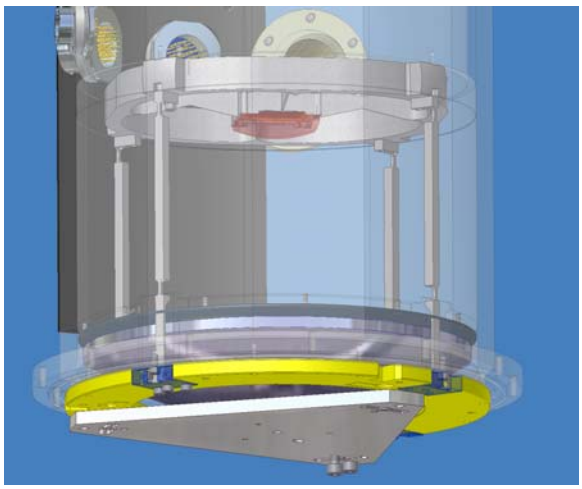

Figure 7: solid model of VIRUS-P camera, showing the mirror mount and adjuster at the lower part of the assembly, invar spacing, rods, and the detector assembly. The detector mount is a stainless steel spider designed for minimum obstruction of light. The field flattener lens has a red color in this rendering and is mounted to the center of the spider.

Figure 8: detector mount assembly. In this orientation, the field flattener is on the underside and the detector is facing downwards. The cold link and flex circuit for detector signals are aligned above one of the spider vanes. A blackened cap (not shown) mounts over the cold block and header board assembly, to prevent reflection light that falls on the central hub.

3.5 Camera and Detector System

Design of the VIRUS-P camera is covered in detail in Ref. 18. The camera is an evacuated Schmidt design, with the detector at the internal focus (Fig. 7). It has f/1.33 for the nominal pupil size of 115 mm, and accepts light from a 125 mm diameter pupil with little vignetting. The optics consist of the fused silica window which has an aspheric front surface (maximum deviation 0.3 mm), the spherical mirror, and the fused silica field flattener with a spherical front and aspheric back surface. The detector and field flattener are suspended in the beam, causing approximately 23% areal obstruction, on axis (for 115 mm diameter input pupil). The excellent FRD performance of the fibers results in the preservation of the central obstruction from the telescope and hence reduces the effect of the detector obstruction to some extent. Otherwise the design has very high efficiency, and produces superb images. High quality images are required so as to maintain sufficient separation between the spectra from individual fibers on the detector, to allow clean extraction of the spectra and maximize the number of fibers per spectrograph.

The CCD has 2k x 2k with 15 μm pixels. Working into the near-UV, low readout noise and good UV-blue QE are important considerations. Available detectors from Fairchild (model 3041) and E2V (CCD230-42) can meet the needs of the instrument, as could a custom foundry run. The prototype originally used an existing older CCD from Orbit. It had higher readout noise (around 6 electrons at 100 kpxl/s) than chips being considered for the final design of VIRUS. Subsequently in summer 2007 the camera was upgraded to use a back-side illuminated Fairchild 3041 detector. Read noise with this system is measured as 4.2 electrons at 100 kpxl/s and 3.6 electrons at 25 kpxl/s with the McDonald Observatory Version 2 CCD controller.

The camera mechanical design (Refs. 17 and 18; Figs. 7 and 8) follows the same principles as for the collimator, using aluminum for the housing and invar metering rods to maintain the focus of the camera mirror with respect to the detector. Flexures between the mirror assembly and the housing provide the radial constraint. The detector and field flattener are suspended in the beam with a stainless spider assembly (Fig 8) that also carries the cold link and flex circuit. The design has been optimized for minimum obstruction. Flexures incorporated into the spider design decouple the expansion of the aluminum housing from the detector head position[17,18]. The field flattener is mounted to the spider with clips at each corner. The CCD package is clamped to the cold block with clips, and a frame of Ultem 1000 polyetherimide provides thermal isolation from the rest of the spider assembly.

3.6 Optical Alignment

The procedure for aligning the optics of VIRUS-P is quite simple. It starts with the alignment of the collimator to the axis of the integral field unit central fiber. This is done using a laser aligned normal to the IFU mount plate, and centered on a cross hair scribed into a Perspex target that is coincident with the center of the IFU. Once this axis is established, the collimator mirror is adjusted in tip and tilt to return the laser on the same axis. The fold mirror in the collimator is initially set to its nominal axial position, and set up to align the slot with the IFU head. It was then adjusted in tip and tilt to direct the laser light to a target coincident with the center of the grating diffractive surface, on a target inserted in the grating holder. It turned out that if the cross hair on the Perspex target is used in the beam, the resulting diffraction pattern produces a cross that can be used to align these optics within the tolerances. The final alignment of the collimator is in focus, which was achieved using a SLR camera with a 200 mm f/1.8 Canon lens set to infinity. The collimator mirror axial position was adjusted to focus the camera on the IFU fiber ends.

The camera setup relies on accurate positioning of the detector and field flattener in the detector spider assembly, to establish the optical axis. With the chip carriers of the Orbit and Fairchild detectors, the positioning of the detector surface proved to be an interactive adjustment, with the Ultem 1000 frame being sanded to set the axial position and tilt of the detector surface. A measuring microscope was used to establish the best-fit plane to the surface of the detector, and to set the detector relative to the seat for the field flattener and the mounting points for the detector spider assembly.

Final adjustment of the optical system was done with the camera evacuated and the detector cold. The camera mirror provides the final adjustment to align and focus the instrument. An adjuster back is used with vacuum feed-throughs to adjust and clamp the mirror position in tip, tilt and piston. Feedback is provided by observing spectral emission line lamps illuminating the IFU, and the image quality is analyzed as a function of fiber position and wavelength to provide the best overall focus, and alignment of the spectra on the detector. This is quite a lengthy and interactive procedure, but provided very good image quality while maintaining all the fibers on the detector. Interchange of IFUs showed a shift of less than a resolution element in fiber position. Alignment of the spectrum of the central fiber with rows on the detector was done by rotating the camera in its mount to the collimator and grating assembly. Alignment of wavelengths to the columns required a small amount of rotation of the grating in its cell.

3.7 Telescope Interface

VIRUS-P mounts primarily at the bent Cassegain f/9 focus of the 2.7 m Harlan J. Smith Telescope at McDonald Observatory. Figure 1 shows the instrument mounted on the telescope, and Ref. 17 gives more details of the mechanical design. In order to provide a gravity-invariant mount location for VIRUS-P, to simulate the conditions that the full VIRUS array will operate under, it is mounted in a gimbal. The gimbal allows VIRUS-P to hang, aligned by gravity in a single vertical direction as the telescope tracks for +/-60 degrees in any direction from zenith. The gimbal mounts to a yolk supported by the main mount plate of the instrument. The IFU is routed in an Igus E-Chain cable carrier to take up the motion of the instrument in the gimbal, and mounts to a f/3.65 telecentric, focal reducer consisting of two doublets, housed in the focal plane assembly. A Uniblitz shutter is installed before the IFU as VIRUS P has no internal shutter. The focal plane assembly also has a fixed pick off mirror feeding an f/3 focal reducer and a commercial thermo-electrically cooled camera for guiding. A broad band B+V filter bandwidth limits the wavelengths for the guide focal reducer.

Setup of the focal plane assembly first required alignment with an autocollimator against the secondary mirror, followed by establishing the focus using a knife-edge mounted to the IFU focal reducer, set to be coincident with the input focus of the IFU fiber bundle. The relative position of the IFU and guide-field centers has been established with astrometry of star fields. Positions of individual objects are recovered to better than 0.7 arcseconds accuracy (80% of samples) with 95% better than 1.0 arcseconds.

3.8 Observing with VIRUS-P

The large 4.55 arcminute guide field provides many guide stars even at high galactic latitudes. During observations, automatic scripts offset the telescope and move guide fiducials to map out the dither pattern required to fill in the area of the IFU. At the 2.7 m we typically do two sets of 3-position dithers, with the second set offset to center a fiber on the intersection of fiber positions in the first set, thereby gaining some spatial resolution and ensuring that any irregularities in the fiber layout pattern are filled in. Integration times for our deep survey observations are typically 3x1200 seconds per position, with a sequence taking 6.5 hours including setup and overheads. The data are sky-noise dominated over

most of the wavelength range in about 100 seconds, and over the full range in 1200 seconds. High-accuracy reconstruction of the photometry with the 1/3 fill-factor IFU requires knowledge of the positions of the fibers on the sky, the size of the image, and the transmission of the atmosphere. Guide images are saved to provide measures of the position, image quality and relative transparency throughout the observation. Corrections applied to standard star observations based on this information allow 10% repeatability of absolute spectrophotometry to be achieved, with the system response shape being stable to a few percent.

3.9 Data Reduction Software

The software for VIRUS must process a highly parallel data stream, quickly, and detect single-line objects, reliably. Development of the final software pipeline for reduction of VIRUS data is being led by MPE. Since VIRUS is naturally a parallel instrument, all the requirements for and attributes of the software can be developed and tested on the prototype. This was a key motivation for the deployment of VIRUS-P on the telescope early in the project. Two pipelines have been developed, one in Texas called VACCINE and the other in Munich, called CURE. VACCINE has been used primarily to reduce and analyze data from the pilot survey on the McDonald 2.7 m, while the algorithms of CURE are tuned for use on the HET. The difference is driven primarily by the plate scale difference between the telescopes. On the 2.7 m the fibers are significantly larger than the image size, while on HET they are comparable. This leads to differences in the detection algorithm. Care is being taken to propagate errors and avoid interpolation through resampling of data which leads to position-dependent smoothing and can alter the noise characteristics. CURE uses a Bayesian detection algorithm that assigns a likelihood of a source to every (spatial and spectral) resolution element. Tests show robust rejection of cosmic rays and reliable detection of 5-σ line flux objects, as required for HETDEX. We have also demonstrated sky subtraction to the Poisson noise limit, with both pipelines, aided by the fact that most of the fibers of VIRUS are observing sky in any exposure.

4. PERFORMANCE OF VIRUS-P

VIRUS-P has been in use since October 2006. It has been used primarily on the McDonald 2.7 m Smith Reflector for a pilot survey to study the properties of Lyman-α emitting (LAE) galaxies. In March 2008 we took the instrument to the HET for the first of a series of tests of its performance to verify predicted sensitivities. More tests will be needed to verify that LAEs are detected at the expected rate, but the first tests resulted in a successful deployment of the instrument and were able to detect faint LAEs and continuum objects.

4.1 Image Quality

For VIRUS-P, the fiber resolution element is reimaged to 4.9 pixels. Image quality delivered by the VIRUS-P optics is excellent. Figure 8 shows that the requirement of 5.0 pixels FWHM or better is met everywhere on the detector. There is a small tilt in focus in the spatial (Y) dimension, which is seen in these plots. At 7.8 pixel spacing between fibers, the 246 fibers of the IFU are accommodated on the detector, with adequate separation to cleanly extract the spectra of each fiber, as demonstrated by the cross cuts in Fig. 9.

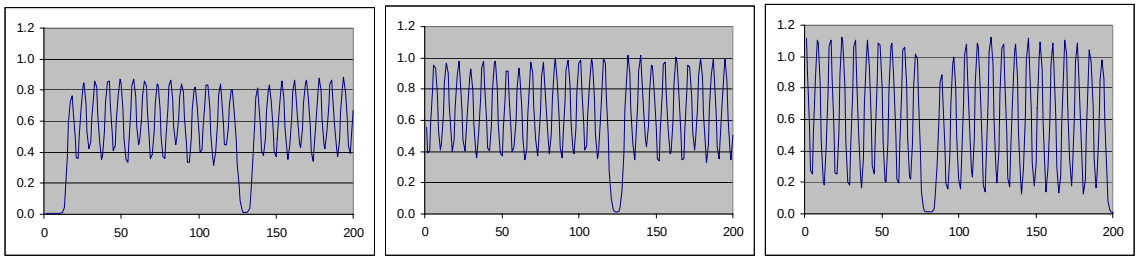

Figure 9, cross cuts in the spatial dimension, demonstrating the image quality and separation of spectra between fibers. The left panel is at the bottom of the frame where the image quality in this dimension is a little worse. The middle panel is at the center of the frame where image quality surpasses specification, and the right panel is at the top of the frame where the image quality in this dimension is the best. Note that the separation of the spectra improves to the top of the frame as expected, with them crossing at 15-20% of the peak, compared to at about 50% of peak at the bottom of the frame. Note also that the scattered light is very low, with the counts approaching bias in the one-fiber gaps between fiber banks.

Scattered light levels in VIRUS-P are very low. At the output of the IFU, the fibers are arranged with gaps between banks, so as to provide a measure of scattered light. Scattered light levels are low enough that the counts are not significantly different from bias in these gaps. We have observed two types of ghosts associated with the grating and the optical configuration[12]. The first is the known "narcissus" ghost discussed in Ref. 19. Narcissus occurs in a spectrograph when light traveling the designed path reflects from the CCD, diffracts again through the dispersion element, and returns to the CCD. In the specific case where the dispersion orders of each pass are identical, the stray light is called a "Littrow ghost". In this case, which we observe, there is no dispersion in the final ghost. Although we are not usually operating with the Littrow wavelength centered in our bandpass, the wavelength is still within our bandpass so the Littrow ghost gets imaged. The other source of stray light is seen when we take neon arc lamp frames. Neon has a large number of bright emission lines that should lie redward of our wavelength range setting. The pattern of these red lines is superimposed on the proper neon spectrum, but with double dispersion and double the expected curvature. This ghost has been largely eliminated with baffling, and is not usually seen in on-sky data. The stray light path we have found that can cause this behavior involves two reflections between the camera window and the grating followed by another first order diffraction of the light. This ghost can be suppressed by specifying high quality AR coatings with coverage to sufficiently long wavelengths that the red light is not reflected efficiently. It is geometry specific, but will be a feature of any grating-camera system where the first camera element is nearly flat. We are looking at ways to suppress these features further in the production design of the VIRUS unit spectrographs.

4.2 Throughput and Sensitivity

Throughput has been measured on spectrophotometric standard stars at the 2.7 m on many photometric nights, and at the HET on two good nights (Fig. 10). Throughput is defined as the fraction of photons incident upon a uniformly filled aperture equivalent to the diameter of the telescope in the upper atmosphere, and includes all losses (atmosphere, telescope reflectivity and obstruction, IFU and optics transmission, and detector QE), but not the aperture effects of the fiber pattern. Throughput is measured by summing all the fibers from the three exposures in a dither pattern in which light is seen from the star, and then correcting for the fraction of light expected to be lost between the fibers in the dither pattern as the 1/3 fill-factor of the fibers is filled in with thee observations. At the 2.7 m, with the VP1 fiber bundle, variations in throughput are seen due to the positioning of the fiber pattern relative to the star and in particular due to the fact that the separations of the hexagonal close-packed fiber array are too large by 6%, and to slight irregularities in the fiber placement, which result in gaps as large as an arcsecond where light can be lost. The relative positions of the fibers are well known and the pointing centers are monitored with the guider, so corrections can be made. Corrections are also made for variations in transparency during a set of dithers on a standard star. When such corrections, on the order of 20% are applied, the throughput is very repeatable (within 10%), and the shape of the response with wavelength is within 2% at all wavelengths. The repeatability of the shape of the throughput curve from measurement to measurement is thus extremely good without an atmospheric dispersion corrector.

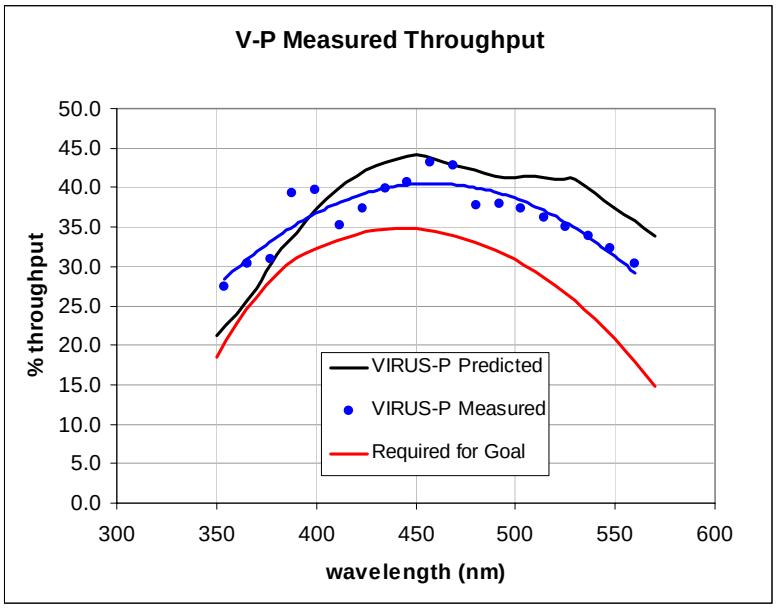

Figure 10: Throughput of VIRUS-P inferred from measurements on the 2.7 m. When corrections are made for the telescope and atmosphere transmission, the inferred throughput of VIRUS-P absent the aperture size of the fiber is derived (blue points). The predicted throughput based on measurements of individual components is shown in black, and agrees quite well with the measurement. The red curve is the required throughput to meet the goals of HETDEX, assuming the upgraded HET meets its specified throughput.

Throughput of VIRUS as a function of wavelength (ignoring aperture effects at the input to the fibers) peaks at 40% and is 30% at 350 nm with 15 m long fibers, in line with predictions based on the measured throughputs of individual components. On-sky, including the atmosphere, the throughput peaks at 18%. This performance exceeds that required for HETDEX. At the 2.7 m the 5-σ point source line flux sensitivity is ~$5x10^{-17}$ erg/cm^2/s, in 2 hours observing under good conditions, in line with predictions[9].

4.3 Stability

The stability of the spectrograph alignment to changes in temperature is excellent. As an example, we monitored the change in position of the spectra on the detector over a night with a 12 Celsius temperature change. The shift in image position is 0.25 pixels (1/20 of a resolution element) for this large temperature change. When deployed on the HET, VIRUS will be in an enclosure but the temperature will not be tightly regulated, so the design meets the requirement of less than 1/10 of a resolution element shift over the temperature range to be encountered in operation. In practice, calibrations are obtained every night, so stability within a night is the overriding requirement, and this is met easily.

5. SCIENCE

VIRUS-P has been designed as a test-bed for the HETDEX project, but has many scientific applications. Since it is designed for the HET, the fibers project to a large area on the sky when fed at the same focal ratio, and the field coverage of the IFU is the largest of any IF spectrograph. The fiber size limits the sensitivity for point sources, but makes VIRUS-P the most sensitive instrument for observing faint low-surface brightness light in extended objects such as the outskirts of galaxies. The other feature that stands out is the coverage into the UV, and VIRUS-P operates significantly blueward of any other integral field spectrograph.

VIRUS-P is being used for an extensive survey of the properties of LAE galaxies, in order to better understand their evolution and large-scale clustering in preparation for HETDEX. To date we have surveyed 134.4 arcmin^2 on the COSMOS, MUNICS-S2, and GOODS-N fields. Analysis of 40 arcmin^2 area on the COSMOS field detected 99 unique emission line sources, of which half are LAEs and half are low redshift emitters[9]. Examples of emission line galaxies detected in this survey are given in Fig. 11. This survey is providing confirmation that we can discriminate LAEs from low redshift galaxies using an equivalent width cut. One remarkable aspect of this survey, which will continue for another year and yield about 300 LAEs with $2 < z < 3.6$, is that VIRUS-P allows the detection of these emission line objects on such a small telescope. When first discovered after a significant period of unsuccessful searches, LAEs required long exposures through narrow band filters on the largest telescopesREF. The volume surveyed by VIRUS-P is so large and the sensitivity offered by spectroscopy over narrow band imaging is sufficient that every 3 square arcminute area field contains several LAEs.

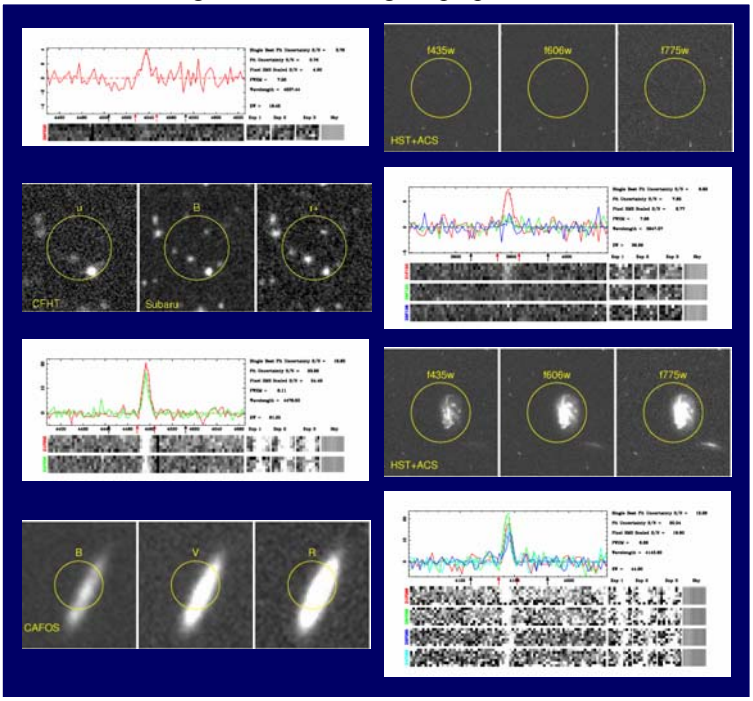

Figure 11, examples of emission line galaxies detected with VIRUS-P on the McDonald 2.7 m as part of the HETDEX pilot survey. Spectra from all fibers where a line detection is made are presented, along with images from the Subaru Telescope, CFHT, and HST. The upper pair are high redshift LAEs and the lower pair are low redshift [OII] emitters

Another application of the sensitivity of VIRUS-P to low surface brightness emission is observation of giant Ly-α halos associated with radio galaxies and Ly-α blobs (LABs) at high redshift. A survey is being undertaken of extended Ly-α emission in radio galaxies that

promises to provide direct tests of models for these 100 kpc scale structures. Initial observations show that VIRUS-P can detect faint extended emission at levels comparable to narrow band images on the largest telescopes, and provides kinematic information at the same time.

The combination of large field of view, large fibers, and coverage to the UV makes VIRUS-P the premier instrument for observing the dynamics and stellar populations in the outskirts of large elliptical galaxies. For example, observations of brightest cluster elliptical galaxies have reached 4 effective radii very easily, an observation that has proven challenging with conventional spectrographs on the largest telescopes. A higher dispersion grating is on order to allow observations to resolve the velocity structure in smaller galaxies as well.

6. SUMMARY AND FUTURE DEVELOPMENT

Evaluation of the performance of VIRUS-P both from an engineering and scientific point of view shows that this instrument has been very successful in meeting the requirements laid out in section 2. Not only is it a very effective and powerful integral field spectrograph in its own right, but it has provided a direct verification that the design basis for the VIRUS array is solid.

Evolution of the design of VIRUS from the prototype to the production model will be made in two steps. First a pre-production prototype will be developed that incorporates the production engineering to reduce costs. Production engineering is being done in collaboration with the Advanced Research Lab (ARL) at Penn State University. VIRUS-PP will be evaluated and used as a test bed for alignment fixturing to prove the production, assembly, and alignment model for the instrument. Its performance will be evaluated on sky and compared with that of VIRUS-P. Following incorporation of any design modifications gleaned from this experience we will enter production with an initial batch of 10 units, followed by full production. Production design of VIRUS is covered in more detail in Ref. 4.

The scientific applications of VIRUS-P have proven varied, and have included observations of planetary nebulae, spiral galaxies, and comets. The instrument is in great demand during dark time on the 2.7 m, and VIRUS-P has revitalized the scientific use of this relatively small telescope. An instrument like VIRUS-P is very powerful on 2 m class telescopes, and our development work on the VIRUS array offers the prospect that similar units can be produced sufficiently cheaply that their use on many existing smaller telescopes would be affordable. Then the instrument would truly be living up to its acronym, spreading widely through the astronomical community!

ACKNOWLEDGEMENTS

We thank the staffs of McDonald Observatory, HET, USM, MPE, and AIP for their help with the construction and deployment of VIRUS-P. VIRUS-P was funded by a gift from the George and Cynthia Mitchell Foundation. The HETDEX pilot survey is funded by the Texas Advanced Research Program under grants 003658-0005-2006 and 003658-0295-2007. HETDEX is led by the University of Texas at Austin with participation from the Max-Planck-Institut für Extraterrestriche-Physik (MPE), Pennsylvania State University, the Astrophysikalisches Institut Potsdam (AIP), Texas A&M University, and the HET consortium.

REFERENCES

1. G.J. Hill, P.J. MacQueen, C. Tejada, P.J. Cobos, P. Palunas, K. Gebhardt, & N. Drory, "VIRUS: a massively-replicated IFU spectrograph for HET," *Proc. SPIE*, **5492**, 25, 2004
2. G.J. Hill, P.J. MacQueen, P. Palunas, A. Kelz, M.M. Roth, K. Gebhardt, & F. Grupp, "VIRUS: a hugely replicated integral field spectrograph for HETDEX", *New Astronomy Reviews*, **50**, 378, 2006
3. G.J. Hill, P.J. MacQueen, J.R. Tufts, A. Kelz, M.M. Roth, W. Altmann, P. Segura, M. Smith, K. Gebhardt, & P. Palunas, "VIRUS: a massively-replicated IFU spectrograph for HET," *Proc. SPIE*, **6269**, paper 6269-93, 2006
4. G.J. Hill, P.J. MacQueen, P. Palunas, S.I. Barnes, M.D. Shetrone "Present and future instrumentation for the Hobby-Eberly Telescope", Proc. SPIE, **7014**-5, 2008
5. S. Faber *et al*., "The DEIMOS spectrograph for the Keck II Telescope: integration and testing," Proc. SPIE, **4841**, 1657, 2003
6. O. Le Fevre *et al*., "VIMOS and NIRMOS multi-object spectrographs for the ESO VLT," Proc. SPIE, **4008**, 546, 2000

7. R.M. Bacon “Probing unexplored territories with MUSE: a second generation instrument for VLT”, *Proc. SPIE*, **6269**, 19, 2006
8. G.J. Hill, & P.J. MacQueen, “VIRUS: an ultra cheap 1000-object IFU spectrograph”, Proc. SPIE, **4836**, 306, 2002
9. G.J. Hill, K.Gebhardt, E. Komatsu, N. Drory, P.J. MacQueen, J.J. Adams, G.A. Blanc, R. Koehler, M. Rafal, M.M. Roth, A. Kelz, F. Grupp, J. Murphy, P. Palunas, C. Gronwall, R. Ciardullo, R. Bender, U. Hopp, D.P. Schneider, “The Hobby-Eberly Telescope Dark Energy Experiment (HETDEX): Description and Early Pilot Survey Results”, in *Panoramic Surveys of the Universe*, *ASP Conf. Series*, in press (arXiv:0806.0183v1), 2008
10. G.J. Hill, H. Nicklas, P.J. MacQueen, C. Tejada de V., C., F.J. Cobos D. & W. Mitsch, "The Hobby-Eberly Telescope Low Resolution Spectrograph", in *Optical Astronomical Instrumentation*, S. D'Odorico, Ed., Proc. SPIE **3355**, 375, 1998.
11. J.D. Murphy, P. Palunas, F. Grupp, P.J. MacQueen, G.J. Hill, A. Kelz, M.M. Roth, “Focal ratio degradation and transmission in VIRUS-P optical fibers”, Proc. SPIE, **7018**-104, 2008
12. J.J. Adams, G.J. Hill, and P.J. MacQueen, “Volume Phase Holographic Grating Performance on the VIRUS-P Instrument”, *Proc. SPIE*, **7014**-258, 2008
13. e.g. J.R. Allington-Smith *et. al*., “Integral Field Spectroscopy with the Gemini Multiobject Spectrograph. I. Design, Construction, and Testing”, PASP, **114**, 892, 2002
14. S.C. Barden & M.A. Wade, “DensePak and spectral imaging with fiber optics”, in *Fiber optics in astronomy*; Proceedings of the Conference, Tucson, AZ, Apr. 11-14, 1988 (A90-20901 07-35). San Francisco, CA, Astronomical Society of the Pacific, 1988, p. 113-124
15. A. Kelz, S.M. Bauer, F. Grupp, G.J. Hill, E. Popow, P. Palunas, M.M. Roth, P.J. MacQueen, & U. Tripphahn, “Prototype development for the integral-field unit for VIRUS”, Proc. SPIE, **6273**, paper 6273-151, 2006
16. e.g. J. Schmoll, M.M. Roth, & U. Laux, “Statistical Test of Optical Fibers for Use in PMAS, the Potsdam Multi-Aperture Spectrophotometer,” PASP, **115**, 854, 2003
17. M.P. Smith, G.J. Hill, P.J. MacQueen, W. Altman, J.A. Goertz, J.M. Good, P.R. Segura, G.L. Wesley, “Mechanical design of VIRUS-P for the McDonald 2.7m Harland J Smith Telescope”, Proc. SPIE, **7014**-259, 2008
18. J.R. Tufts, P.J. McQueen, M.P. Smith, P.R. Segura, G.J. Hill, R.D. Edmonston, “VIRUS-P: camera design and performance”, *Proc. SPIE*, **7021**-10, 2008
19. E.B. Burgh, M.A. Bershady, K.B. Westfall, and K.H. Nordsieck, “Recombination Ghosts in Littrow Configuration: Implications for Spectrographs Using Volume Phase Holographic Gratings,” PASP **119**, 1069, 2007
20. L.L. Cowie & E.M. Hu, “High-z Ly-alpha Emitters. I. A Blank-Field Search for Objects near Redshift Z = 3.4 in and around the Hubble Deep Field and the Hawaii Deep Field SSA 22”, *AJ*, **115**,1319, 1998